Electronic structure of Eu atomic wires encapsulated inside single-wall carbon nanotubes

Ryo Nakanishi,[1] Ryo Kitaura,[1] Paola Ayala,[2] Hidetsugu Shiozawa,[2] Kathrin de Blauwe,[2] Patrick Hoffmann,[3] Daeheon Choi,[1] Yasumitsu Miyata,[1] Thomas Pichler,[2] and Hisanori Shinohara[1]

[1]*Department of Chemistry & Institute for Advanced Research, Nagoya University, Nagoya, 464-8602, Japan*

[2]*Faculty of Physics, University of Vienna, A-1090 Wien, Austria*

[3]*BESSY II, D-12489 Berlin, Germany*

(Received 3 May 2012; revised manuscript received 11 August 2012; published 26 September 2012)

X-ray absorption (resonant) photoelectron spectroscopy has been employed to investigate electronic structure of Eu atomic wires encapsulated in single-wall carbon nanotubes (SWCNTs). The measurements reveal that there is a substantial electron transfer of $+1.79 \pm 0.11$ from a Eu atom to the surrounding SWCNT. The shape of the observed Fermi edge is different from that of a three-dimensional metal, suggesting that electrons in this one-dimensional system form a Tomonaga-Luttinger liquid.

DOI: 10.1103/PhysRevB.86.115445 PACS number(s): 73.63.Fg, 71.10.Hf, 78.70.Dm, 79.60.−i

I. INTRODUCTION

Single-wall carbon nanotubes (SWCNTs) are one-dimensional (1D) conductors with unusual transport properties. Their novel electronic properties result from the unique structure of a graphene sheet with sp^2 hybridization that is rolled up to a narrow tube. Not surprisingly, a large variety of functionalities has been envisaged through the functionalization of the inner and/or outer wall. Three major ways for functionalization are classified as exohedral attachment, substitutional (on wall), and endohedral functionalization (filling).[1–16] Filling, especially, can encompass a large number of possibilities, depending on the materials filled inside SWCNTs, which can provide new functional SWCNTs as well as novel hybrid materials that have a specific low-dimensional structure and properties.

In this respect, a low-dimensional molecular array,[1–7] long linear carbon chains,[8–10] and metal complex nanowires[11–16] have been synthesized inside carbon nanotubes (CNTs) and studied during the past decade. Recently, we have added a new family of low-dimensional nanomaterials formed in CNTs, i.e., metal atomic wires (AWs) that were synthesized by a direct nanofilling reaction.[17] The metal AWs, obtained by this method, possess a diameter of one to several atoms, whose structure and magnetization behavior are distinctly different from those of bulk crystals. Recently reported density functional theory (DFT) band structure calculation of the metallic AWs encapsulated in CNTs (AW@CNTs) suggested that there is a significant electron transfer from metallic AWs to CNT and that the electronic structure of AW@CNTs could not be explained as a simple superposition of neutral AW and CNTs.[18–20] To understand the basic properties of this new class of low-dimensional systems in CNTs (AW@CNTs) and to elucidate their electronic structure, it is crucial to investigate the interaction exerted between the encapsulated AW and the CNT.

Photoelectron spectroscopy (PES) using synchrotron radiation is a very powerful tool to explore the electronic structure of nanomaterials. For example, x-ray photoelectron spectroscopy (XPS) and x-ray absorption spectroscopy (XAS) have been applied to CNTs and hybrid CNTs, where detailed information on the electronic structure, including the bonding nature of carbon, interaction between encapsulated species and CNTs, and the existence of the Tomonaga-Luttinger liquid (TLL) in CNTs, have been elucidated.[21–29] Here, we have applied synchrotron resonant PES (RESPES) and XAS to explore the electronic structure of Eu AWs encapsulated in SWCNTs [Eu(AW)@SWCNTs]. By using these techniques, we have determined the degree of charge transfer and the bonding environment of carbon in Eu(AW)@SWCNTs. The results show that SWCNTs acquire a large negative charge originating from the encapsulated Eu(AW) and that the extent of charge transfer from Eu(AW) to SWCNTs determined experimentally is consistent with the corresponding DFT calculations.[19] Furthermore, the shape of the Fermi edge revealed by low-temperature XPS measurements is different from that of bulk three-dimensional (3D) metal, suggesting that the electronic structure of Eu(AW)@SWCNTs is not a normal 3D metal.

II. EXPERIMENTAL

The Eu(AW)@SWCNTs were synthesized by the direct nanofilling method as described in our previous report.[17] We used Meijo SO SWCNTs, which are known to have a narrow diameter distribution (1.4 ± 0.1 nm), as a template for the preparation of Eu(AW). Due to the narrow diameter distribution of the SWCNTs used, the Eu(AW) formed inside have an almost uniform diameter. After vacuum annealing at 873 K to remove residual Eu atoms attached on the tubes, the samples were further washed by using diluted HCl to remove the residual Eu atoms. The structure of Eu(AW)@SWCNTs was observed by a JEM-2100F (JEOL) high-resolution transmission electron microscopy (TEM) operated at 80 keV at room temperature. For the XAS and XPS studies, the samples were dispersed in 1,2-dichloroethane with ultrasonication for 1 h, and then the dispersion solution was sprayed onto a 5×7 mm sapphire (0001) substrate in order to make thin films of Eu(AW)@SWCNTs. The sample substrates were placed on a Mo sample holder, and prior to the measurements the substrates were annealed at 573 K in 5×10^{-8} Pa.

The spectroscopy experiments were performed at a beamline UE52PGM at BESSY II, which has an energy resolution $(E/\Delta E)$ of 1×10^4. The XAS spectra were recorded in partial yield and drain current modes. XPS was performed by using a hemispherical SCIENTA SES 200 photoelectron energy

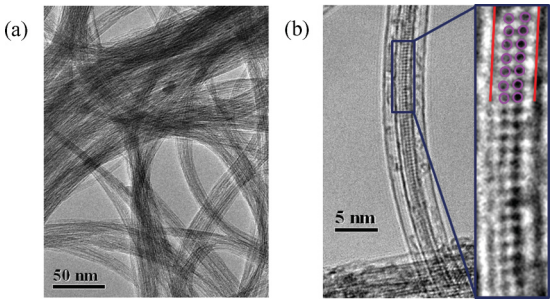

FIG. 1. (Color online) (a) Low-magnification TEM image of Eu(AW)@SWCNTs. (b) High-magnification TEM image of Eu(AW)@SWCNTs (left) and magnified image (right). In the magnified image, red lines correspond to the side wall of SWCNT, and purple circles correspond to the Eu atoms.

analyzer. A base pressure of below 5×10^{-8} Pa was kept for all the measurements.

III. RESULTS AND DISCUSSION

Figures 1(a) and 1(b) show typical TEM images of an HCl-treated Eu(AW)@SWCNTs sample. As clearly seen, crystalline Eu(AW) are formed inside the 1D space of SWCNTs, and no residual Eu atoms were observed on the nanotube surface. Due to the narrow diameter distribution of SWCNTs, most of the Eu(AW) possess a 2×2 structure that is similar to the previously reported Gd wire.[30]

Figures 2(a) and 2(b) show XAS in the C $1s\pi^*$ region of pristine and Eu(AW)@SWCNTs, respectively. A characteristic fine structure in the π^* response is observed, which can be attributed to the Van Hove singularities (VHs) of SWCNTs. To identify these peaks, we employ a line-shape analysis of the fine structure with Voigt functions. The fine structure was

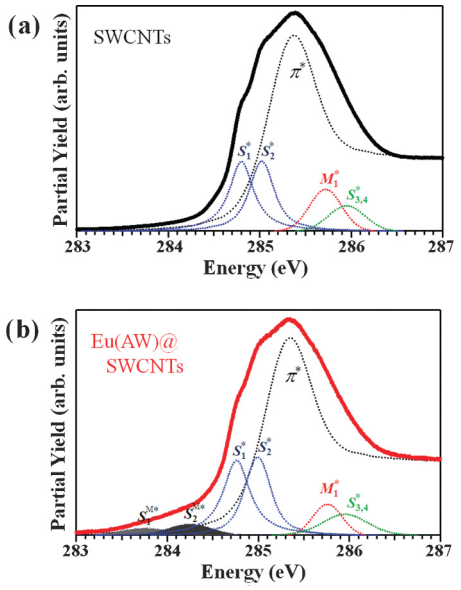

FIG. 2. (Color online) X-ray absorption spectra in the C$1s\pi^*$ region of (a) SWCNTs and (b) Eu(AW)@SWCNTs. The recorded absorption edges (heavy solid lines) are depicted, together with line-shape analysis results, which include corresponding VHs and the overall π^* (dotted lines).

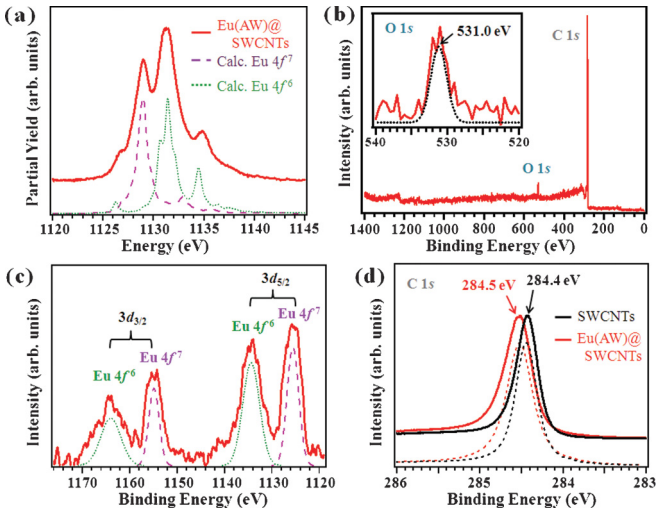

FIG. 3. (Color online) (a) Calculated and observed XAS spectra of the Eu 3*d* edge. (b) XPS survey scan spectrum and (c) the magnified spectrum in the region of the Eu 3*d* core level of Eu(AW)@SWCNTs measured with excitation photon energy of 1500 eV. Inset of (b) shows O 1*s* core level. (d) XPS spectrum in the region of the C 1*s* core level of Eu(AW)@SWCNTs (red) and pristine SWCNTs (black) with excitation photon energy of 400 eV.

represented by four Voigt components. The main π^* peak is centered at 285.4 eV, and the four main fine-structure peaks are positioned at 284.8, 285.0, 285.7, and 286.0 eV, which are assigned to S_1^*, S_2^*, M_1^*, and $S_{3,4}^*$, respectively, according to the previous reports.[29,31–34] By comparing these peaks to the pristine and Eu(AW)@ SWCNTs samples, a small decrease of the peak related to the S^* was observed. This can be attributed to electron transfer from Eu(AW) to SWCNTs, in which the VHs located at bottom of valence band of semiconducting tubes are partially filled. This is in very good agreement with the previous studies of XPS on electron doped SWCNTs.[3,29,31] In the case of Eu(AW)@SWCNTs, additional fine structures appear at 283.9 and 284.2 eV, which are assigned to S_1^{M*} and S_2^{M*}, respectively. These peaks can be attributed to the VHs of the semiconducting tubes strongly screened by the encapsulated Eu(AW) as extensively discussed in a previous report.[27] This also strongly suggest the existence of the electron transfer from Eu(AW) to SWCNTs.

The common electronic configurations of europium in the elemental solid and in mixed-valence compounds are Eu^0 ($4f^7\ 5d^0\ 6s^2$), Eu^{2+} ($4f^7\ 5d^0\ 6s^0$), and Eu^{3+} ($4f^6\ 5d^0\ 6s^0$). To investigate the charge state (valency) of Eu inside the Eu(AW)@SWCNTs, we have analyzed the XAS and XPS spectra recorded in the region of the Eu 3*d* core levels. The typical electronic configurations of Eu 4*f* orbital are $4f^7$ or $4f^6$, which can be investigated by $3d \rightarrow 4f$ XAS spectra. Figure 3(a) shows the observed and simulated Eu $3d \rightarrow 4f$ XAS spectra. We used Eu $3d^{10}\ 4f^{\ 7}$ (Eu^0 or Eu^{2+}) and Eu $3d^{10}\ 4f^{\ 6}$ (Eu^{3+}) electronic configurations as the initial state and Eu $3d^9\ 4f^8$ and $3d^9\ 4f^7$ as the final state in the spectral simulation based on the Cowan code.[35] We can clearly see that the experimental XAS spectrum contains components corresponding to the peaks arising from Eu $4f^{\ 7}$ and Eu $4f^6$,

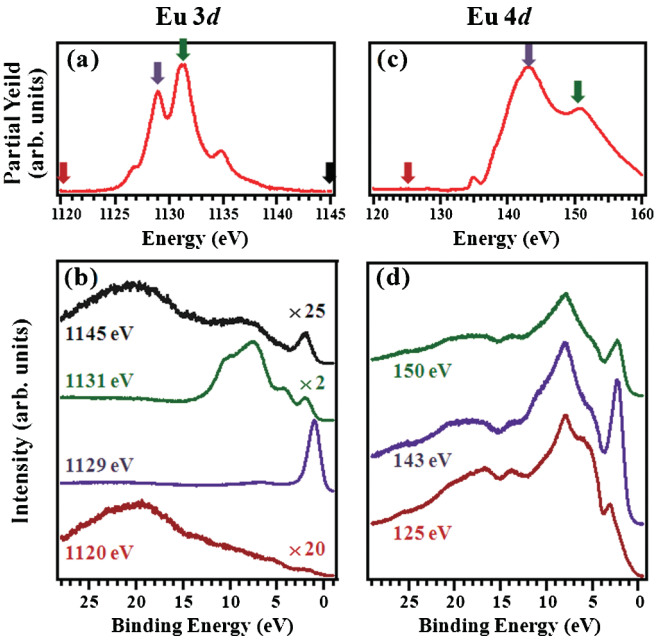

FIG. 4. (Color online) (a) Eu 3*d* absorption edge and (b) RESPES at the energies indicated by the arrows. (c) Eu 4*d* absorption edge and (d) corresponding RESPES at the corresponding energies indicated by the arrow.

indicating that both of this states are present in the Eu atoms encapsulated in the tubes.

To obtain more information on the interaction exerted between Eu and SWCNTs, it is necessary to know the Eu/C atomic ratio in the sample. To estimate the ratio, a wide-range XPS was measured with an excitation energy of 1500 eV, as shown in Fig. 3(b). In addition to the Eu 3*d* peaks observed at 1120 ∼ 1170 eV, a strong C1*s* peak and a small O1*s* peak (see inset) were observed at 284.5 and 531.0 eV, respectively. No contamination from catalyst particles was observed. Figure 3(c) shows a magnified spectrum of the Eu 3*d* peaks.

XPS peaks arising from Eu $4f^7$ and Eu $4f^6$ are clearly discernible. To determine the atomic ratio between Eu $4f^7$, Eu $4f^6$, and carbon, an integration of the peak area was employed by a Gaussian fitting. Considering the photoionization cross section of each transition, a ratio of Eu $4f^6$/Eu $4f^7 = 1.17 \pm 0.06$ and Eu/C $= (8.89 \pm 0.45) \times 10^{-4}$ was obtained.

Figure 3(d) shows XPS spectra of pristine SWCNTs and Eu(AW)@SWCNTs measured in the region of the C1*s* core level with an excitation energy of 400 eV. As seen in the figure, a high-energy shift and broadening of C1*s* peak were observed. Peak fitting using Voigt function reveals that the peak shows a blueshift from 284.4 to 284.5 eV and the increase of the full width at half-maximum from 0.31 to 0.38 after Eu(AW) encapsulation. A similar behavior has been observed in potassium-intercalated SWCNTs,[25] which again suggests that there is an electron transfer from Eu(AW) to SWCNTs.

The panels in Figs. 4 show the Eu XAS M_5 [Fig. 4(a)] and $N_{4,5}$ [Fig. 4(b)] edges of annealed Eu(AW)@SWCNTs. The XAS response is normalized to the background absorbance of clean Au films. The panels in Figs. 4(c) and 4(d) correspond, respectively, to resonance and nonresonance valence-band photoemission spectra recorded at the M_5 and $N_{4,5}$ edges;

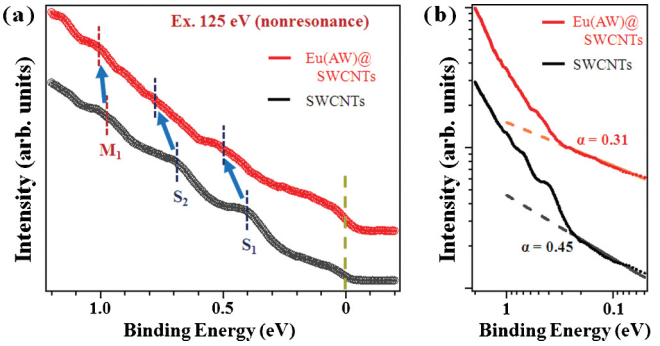

FIG. 5. (Color online) (a) Valence-band x-ray photoelectron spectra of pristine SWCNTs (black) and Eu(AW)@SWCNTs (red) recorded at 125 eV. (b) Double-logarithmic representation of (a) for the analysis of the power law of TLL theory. Linear fit between 0.05 and 0.25 eV, used as derivation of α, are also shown as solid lines.

the excitation energies at which each spectrum was recorded are indicated by arrows in the upper XAS spectra of Fig. 4. The excitation energies are calibrated by the Fermi edge of clean Au.

At the Eu 3*d* RESPES spectrum in resonance with Eu $4f^7$ [purple line in Fig. 4(c), obtained by using 1129 eV photon energy], the Eu 4*f* signal at around 2 eV is strongly resonance enhanced as compared to the carbon response. No prominent changes are observed in the carbon response in the resonance spectrum, suggesting that the degree of orbital hybridization between carbon orbitals and Eu 4*f* orbitals in the Eu(AW) is small. At the Eu 3*d* RESPES spectrum in resonance with Eu $4f^6$ [green line in Fig. 4(b), obtained with 1131-eV photon energy], the Eu $4f^6$ signal is also resonance enhanced, and several peaks arising from the $4f^6$ multiplet are observed. In addition, the intensity of the $4f^7$ signal is reduced since it is above the resonance edge. Both the observed energy separation of the $4f^7$ and the $4f^6$ multiplets are in good agreement with the atomic multiplet calculations. The actual intensities are modified by the resonance enhancement. Essentially the same spectral features are also observed in the *N*-edge resonance spectra [Fig. 4(d)], but they appear much less enhanced due to a strong multiplet interaction between the shallow 4*d* core levels and the localized 4*f* multiplets.[36] This leads to a delocalization of the valence electrons and a less pronounced resonance enhancement.

To reveal the nature of the charge transfer in this system, the density of states (DOS) at the Fermi level was investigated. Figure 5(a) shows the valence band photoemission spectrum of Eu(AW)@SWCNTs around the Fermi edge together with the spectrum corresponding to the pristine SWCNTs used as a reference. These spectra were recorded by using the incident photon energy of 125 eV. The observed DOS at Fermi level of pristine SWCNTs is small, which is consistent with previous reports[22,24,25] and in agreement with the fact that only about 1/3 of the pristine SWCNTs used in this experiment are metallic. Close inspection of the valence-band photoemission spectrum reveals that three peaks arising from VHs (S_1, S_2, and M_1) can be recognized. These salient VHs peaks become visible, provided that the SWCNTs used in this study are clean and possess a narrow diameter distribution. The spectrum corresponding to the Eu(AW)@SWCNTs shows similar

features. However, the DOS at the Fermi edge of Eu(AW)@SWCNTs is slightly larger than that of pristine SWCNTs. This suggests an increased metallicity in the Eu(AW)@ SWCNTs sample compared to the pristine SWCNTs. This increased DOS at the Fermi edge also suggests that the SWCNTs carry a large net charge originating from the Eu(AW) encapsulated inside and that the Eu(AW)@ SWCNTs sample is driven into a metallic state.

To determine the degree of charge transfer, we have focused on the position of S_1, S_2, and M_1 peaks in XAS of Eu(AW)@SWCNTs. The peak position shows a small shift to the higher-energy region consistent with the charge transfer from Eu(AW) to SWCNTs. In the previous reports on potassium- and ferrocene-intercalated SWCNTs[24,26] an empirical equation between the S_1 peak shift, ΔE_f, and the amount of electrons transferred to SWCNTs per one carbon atom, Nc, was suggested as follows:

$$N\,\mathrm{c} = 7.98 \times 10^{-3} \times \Delta E_f - 6.05 \times 10^{-5}. \qquad (1)$$

By using the value of ΔE_f and Eu/C as 0.10 ± 0.02 eV and $(8.89 \pm 0.45) \times 10^{-4}$, respectively, the number of electrons transferred to SWCNTs is calculated to be 0.82 ± 0.04 per one Eu atom. In this calculation, all Eu atoms (both Eu $4f^7$ and Eu $4f^6$) are considered to contribute to the electron transfer. It should be noted that Eu atoms at the end of Eu(AW) are exposed to air and that highly reactive Eu atoms are expected to be oxidized. Actually, our preliminary scanning transmission electron microscopy-electron energy loss spectroscopy (STEM-EELS) measurements have shown that Eu atoms are oxidized to be Eu_2O_3 at the end of Eu(AW).

During the XPS survey scans, we have observed a marginal oxygen peak, which, in the case of pristine CNTs, can be completely eliminated by heat treatment.[5] However, in the present Eu(AW)@SWCNTs, the heat treatment seems not sufficient to eliminate the oxygen observed in the XPS spectrum as shown in Fig. 3(b). In addition, the observed O 1s peak of 531.0 eV shown in inset of Fig. 3(b) has been assigned to the O^{2-} ions of Eu_2O_3 on the surface of oxygen-deficient regions.[37] These results also support the formation of Eu_2O_3 on the edge of Eu(AW). Because Eu atoms in Eu_2O_3 do not contribute to the electron transfer, we have recalculated the amount of electrons transferred to SWCNTs, assuming that the all electron transfer is attributed to Eu^{2+}, which correspond to the Eu $4f^7$ state. Considering Eu $4f^6$/Eu $4f^7 = 1.17 \pm 0.06$, the number of electrons transferred from Eu $4f^7$ to SWCNTs is 1.79 ± 0.11 per one Eu atom, which is in good agreement with a recent *ab initio* calculation of Eu(AW)@SWCNTs.[19]

Finally, we have characterized the electrons in the 1D Eu(AW)@SWCNTs system in terms of the TLL. One of the important features of the TLL state can be characterized by the DOS $n(E)$ near the Fermi level. The DOS shows a power-law dependency of $n(E) \propto (E\text{-}E_F)^{\alpha}$, where α depends on the strength of the Coulomb interaction. As shown previously,[22,24] α can be expressed in terms of a Luttinger parameter g as $\alpha = (g + g^{-1} - 2)/8$. α can be directly derived from a linear fit of the double-logarithmic representation of an XPS spectrum in the low binding energy region [Fig. 5(b)]. For the pristine SWCNTs [black dots and line in Fig. 5(b)], α and g are found to be 0.45 and 0.18, respectively, which is in good agreement with previous results.[22,24] In the case of Eu(AW)@SWCNTs [red dots and line in Fig. 5(b)], α and g are found to be 0.31 and 0.24, respectively. As compared with α and g of pristine SWCNTs, those of Eu(AW)@SWCNTs are reduced, which means that the electronic structure of Eu(AW)@SWCNTs hybrid systems is still 1D but contains additional conduction channels via the Eu(AW) inside the metallic SWCNT. Previous studies show that the heavily electron-doped SWCNTs undergo a transition from a 1D TLL to a 3D Fermi liquid.[24,25,38] If the electrons would form a 3D Fermi liquid, we should expect $\alpha = 0$ and $g = 1$. Since the present values of α and g are not exactly 0 and 1, respectively, we conclude that the electron transfer from Eu(AW) to SWCNTs does not completely destroy the 1D nature of the metallic ground state, where additional conduction channels may emerge in these novel Eu(AW)-filled 1D SWCNT hybrids. This, in fact, is similar to the case of partially potassium-intercalated SWCNTs.[24,25,38]

IV. CONCLUSIONS

Interaction between encapsulated Eu(AW) and SWCNTs is experimentally investigated by synchrotron XPS, RESPES, and XAS. The results show that encapsulation of Eu(AW) causes a large electron transfer of 1.79 ± 0.11 electrons from Eu to the surrounding SWCNTs. Electrons in the 1D Eu(AW) inside SWCNTs appear to form a Tomonaga-Luttinger liquid that differs significantly from the Fermi liquid in a normal 3D metal.

ACKNOWLEDGMENTS

This work has been supported by the Grant-in-Aids for Specific Area Research (Grant No. 19084008) on Carbon Nanotube Nano-Electronics and for Scientific Research S (No. 22225001) of MEXT of Japan. This work was also supported by the Austrian Science Fund through Project No. FWF P21333-N20 and the German Research Foundation through Project No. DFG PI 440-4/5. We acknowledge the Helmholtz-Zentrum Berlin Electron Storage Ring BESSY II for provision of synchrotron radiation at beamline UE52PGM. The research leading to these results has received funding from the EU (FP7/2007-2013) under Grant No. 226716. R.N. thanks the Japan Society for the Promotion of Science for a Research Fellowship for Young Scientists. P.A. was supported by a Marie Curie Intra European Fellowship within the 7th European Community Framework Programme. H.S. thanks the Leverhulme Trust for support through an early career fellowship.

[1] B. Smith, M. Monthioux, and D. Luzzi, Nature **396**, 323 (1998).

[2] K. Hirahara, K. Suenaga, S. Bandow, H. Kato, T. Okazaki, H. Shinohara, and S. Iijima, Phys. Rev. Lett. **85**, 5384 (2000).

[3] T. Takenobu, T. Takano, M. Shiraishi, Y. Murakami, M. Ata, H. Kataura, Y. Achiba, and Y. Iwasa, Nat. Mater. **2**, 683 (2003).

[4]S. Bandow, T. Hiraoka, T. Yumura, K. Hirahara, H. Shinohara, and S. Iijima, Chem. Phys. Lett. **384**, 320 (2004).
[5]H. Shiozawa, H. Ishii, H. Kihara, N. Sasaki, S. Nakamura, T. Yoshida, Y. Takayama, T. Miyahara, S. Suzuki, Y. Achiba, T. Kodama, M. Higashiguchi, X. Y. Chi, M. Nakatake, K. Shimada, H. Namatame, M. Taniguchi, and H. Kataura, Phys. Rev. B **73**, 075406 (2006).
[6]Z. Wang, H. Li, Z. Liu, Z. Shi, J. Lu, K. Suenaga, S. Joung, T. Okazaki, Z. Gu, J. Zhou, Z. Gao, G. Li, S. Sanvito, E. Wang, and S. Iijima, J. Am. Chem. Soc. **132**, 13840 (2010).
[7]T. Okazaki, Y. Iizumi, S. Okubo, H. Kataura, Z. Liu, K. Suenaga, Y. Tahara, M. Yudasaka, S. Okada, and S. Iijima, Angew. Chem. Int. Ed. **123**, 4955 (2011).
[8]X. Zhao, Y. Ando, Y. Liu, M. Jinno, and T. Suzuki, Phys. Rev. Lett. **90**, 187401 (2003).
[9]D. Nishide, H. Dohi, T. Wakabayashi, E. Nishibori, S. Aoyagi, M. Ishida, S. Kikuchi, R. Kitaura, T. Sugai, M. Sakata, and H. Shinohara, Chem. Phys. Lett. **428**, 356 (2006).
[10]C. Zhao, R. Kitaura, H. Hara, S. Irle, and H. Shinohara, J. Phys. Chem. C **115**, 13166 (2011).
[11]P. Ajayan, T. Ebbesen, T. Ichihashi, S. Iijima, K. Tanigaki, and H. Hiura, Nature (London) **362**, 522 (1993).
[12]J. Sloan, D. M. Wright, S. Bailey, G. Brown, A. P. E. York, K. S. Coleman, M. L. H. Green, J. Sloan, D. M. Wright, J. L. Hutchison, and M. L. H. Green, Chem. Commun. (Cambridge) **8**, 699 (1999).
[13]R. Meyer, J. Sloan, R. Dunin-Borkowski, A. Kirkland, M. Novotny, S. Bailey, J. Hutchison, and M. Green, Science **289**, 1324 (2000).
[14]E. Philp, J. Sloan, A. Kirkland, R. Meyer, S. Friedrichs, J. Hutchison, and M. Green, Nat. Mater. **2**, 788 (2003).
[15]L. Li, A. Khlobystov, J. Wiltshire, G. Briggs, and R. Nicholas, Nat. Mater. **4**, 481 (2005).
[16]R. Kitaura, D. Ogawa, K. Kobayashi, T. Saito, S. Ohshima, T. Nakamura, H. Yoshikawa, K. Awaga, and H. Shinohara, Nano Res. **1**, 152 (2008).
[17]R. Kitaura, R. Nakanishi, T. Saito, H. Yoshikawa, K. Awaga, and H. Shinohara, Angew. Chem. Int. Ed. **48**, 8298 (2009).
[18]J. Parq, J. Yu, and G. Kim, J. Chem. Phys. **132**, 054701 (2010).
[19]J. Zhou, X. Yan, G. Luo, R. Qin, H. Li, J. Lu, W. Mei, and Z. Gao, J. Phys. Chem. C **114**, 15347 (2011).
[20]S. Konabe and S. Okada, Appl. Phys. Lett. **98**, 073109 (2011).
[21]M. Bockrath, D. Cobden, J. Lu, A. Rinzler, R. Smalley, L. Balents, and P. McEuen, Nature (London) **397**, 598 (1999).
[22]H. Ishii, H. Kataura, H. Shiozawa, H. Yoshioka, H. Otsubo, Y. Takayama, T. Miyahara, S. Suzuki, Y. Achiba, M. Nakatake, T. Narimura, M. Higashiguchi, K. Shimada, H. Namatame, and M. Taniguchi, Nature (London) **426**, 540 (2003).
[23]H. Shiozawa, H. Rauf, T. Pichler, M. Knupfer, M. Kalbac, S. Yang, L. Dunsch, B. Büchner, D. Batchelor, and H. Kataura, Phys. Rev. B **73**, 205411 (2006).
[24]H. Rauf, T. Pichler, M. Knupfer, J. Fink, and H. Kataura, Phys. Rev. Lett. **93**, 096805 (2004).
[25]C. Kramberger, H. Rauf, M. Knupfer, H. Shiozawa, D. Batchelor, A. Rubio, H. Kataura, and T. Pichler, Phys. Rev. B **79**, 195442 (2009).
[26]H. Shiozawa, T. Pichler, A. Gruneis, R. Pfeiffer, H. Kuzmany, Z. Liu, K. Suenaga, and H. Kataura, Adv. Mater. **20**, 1443 (2008).
[27]H. Shiozawa, T. Pichler, C. Kramberger, M. Rümmeli, D. Batchelor, Z. Liu, K. Suenaga, H. Kataura, and S. R. P. Silva, Phys. Rev. Lett. **102**, 046804 (2009).
[28]T. Pichler, C. Kramberger, P. Ayala, H. Shiozawa, M. Knupfer, M. Rümmeli, D. Batchelor, R. Kitaura, N. Imazu, K. Kobayashi, and H. Shinohara, Phys. Status Solidi B **245**, 2038 (2008).
[29]P. Ayala, R. Kitaura, R. Nakanishi, H. Shiozawa, D. Ogawa, P. Hoffmann, H. Shinohara, and T. Pichler, Phys. Rev. B **83**, 085407 (2011).
[30]R. Kitaura, N. Imazu, K. Kobayashi, and H. Shinohara, Nano Lett. **8**, 693 (2008).
[31]C. Kramberger, H. Rauf, H. Shiozawa, M. Knupfer, B. Büchner, T. Pichler, D. Batchelor, and H. Kataura, Phys. Rev. B **75**, 235437 (2007).
[32]P. Ayala, Y. Miyata, K. De Blauwe, H. Shiozawa, Y. Feng, K. Yanagi, C. Kramberger, S. R. P. Silva, R. Follath, H. Kataura, and T. Pichler, Phys. Rev. B **80**, 205427 (2009).
[33]P. Ayala, H. Shiozawa, K. De Blauwe, Y. Miyata, R. Follath, H. Kataura, and T. Pichler, J. Mater. Sci. **45**, 5318 (2010).
[34]K. De Blauwe, D. J. Mowbray, Y. Miyata, P. Ayala, H. Shiozawa, A. Rubio, P. Hoffmann, H. Kataura, and T. Pichler, Phys. Rev. B **82**, 125444 (2010).
[35]R. D. Cowan, J. Opt. Soc. Am. **58**, 808 (1968).
[36]H. Ogasawara, A. Kotani, and B. T. Thole, Phys. Rev. B **50**, 12332 (1994).
[37]P. Zhang, Y. Zhao, T. Zhai, X. Lu, Z. Liu, F. Xiao, P. Liu, and Y. Tong, J. Electrochem. Soc. **159**, D204 (2012).
[38]H. Rauf, H. Shiozawa, T. Pichler, M. Knupfer, B. Büchner, and H. Kataura, Phys. Rev. B **72**, 245411 (2005).